Diffusion of Cholesterol and Its Precursors in Lipid Membranes Studied by ^{1}H Pulsed Field Gradient Magic Angle Spinning NMR

Holger A. Scheidt,*‡ Daniel Huster,*† and Klaus Gawrisch‡

*Junior Research Group, "Solid-State NMR Studies of Membrane-Associated Proteins", Biotechnological-Biomedical Center and †Institute of Medical Physics and Biophysics, University of Leipzig, D-04107 Leipzig, Germany; and ‡Laboratory of Membrane Biochemistry and Biophysics, National Institute on Alcohol Abuse and Alcoholism, National Institutes of Health, Bethesda, Maryland 20892

ABSTRACT Cholesterol content is critical for membrane functional properties. We studied the influence of cholesterol and its precursors desmosterol and lanosterol on lateral diffusion of phospholipids and sterols by ^{1}H pulsed field gradients (PFG) magic angle spinning (MAS) NMR spectroscopy. The high resolution of resonances afforded by MAS NMR permitted simultaneous diffusion measurements on 1,2-dipalmitoyl-*sn*-glycero-3-phosphocholine (DPPC) and sterols. The cholesterol diffusion mirrored the DPPC behavior, but rates were slightly higher at all cholesterol concentrations. DPPC and cholesterol diffusion rates decreased and became cholesterol concentration dependent with the onset of liquid-ordered phase formation. The activation energies of diffusion in the coexistence region of liquid-ordered/liquid-disordered phases are higher by about a factor of 2 compared to pure DPPC and to the pure liquid-ordered state formed at higher cholesterol concentrations. We assume that the higher activation energies are a reflection of lipid diffusion across domain boundaries. In lanosterol- and desmosterol-containing membranes, the DPPC and sterol diffusion coefficients are somewhat higher. Whereas the desmosterol rates are only slightly higher than those of DPPC, the lanosterol diffusion rates significantly exceed DPPC rates, indicating a weaker interaction between DPPC and lanosterol.

INTRODUCTION

Cholesterol is a major constituent of mammalian cell membranes. It is well known that cholesterol is very efficient in altering membrane biophysical properties including membrane lateral compressibility and permeability to solutes (1). Cholesterol also influences lateral organization of membrane constituents, resulting in formation of lipid clusters (2) and so-called rafts (3–5). Lipid-protein interaction (6) and function of membrane-bound proteins (7–9) are also altered by cholesterol. Even slight changes of membrane cholesterol content cause significant, intolerable alterations of membrane properties and may severely affect biological function.

Interactions between cholesterol and phospholipids are responsible for the changes in membrane properties (10). The presence of such interactions at the molecular level is reflected in molecular order parameters of the phospholipid chains. It was observed that lipid chain order strongly increases with increasing cholesterol concentration. The ability of cholesterol to induce those biophysical changes is related to its molecular structure. The cholesterol molecule may form hydrogen bonds to lipid polar groups, including the phosphate group and the carbonyls (11). The van der Waals interactions between hydrocarbon chains and the rigid ring structure of cholesterol could be responsible for the chain order increase.

Biological membranes are liquid-crystalline at physiological conditions, a phase state with rapid lateral lipid diffusion. The aim of this study was to investigate if lateral diffusion rates of matrix phospholipids and cholesterol differ. We chose the phospholipid 1,2-dipalmitoyl-*sn*-glycero-3-phosphocholine (DPPC) as the model because of its closeness in properties to sphingomyelin (SM), a major constituent of membrane rafts (12). Another advantage of DPPC is that its hydrocarbon chains can be easily deuterated. This reduces signal superposition, permitting detection of ^{1}H NMR resonances specific to sterols.

The study was motivated by the ongoing discussion on the specificity of cholesterol-lipid interactions in context with raft formation. Rafts are domains responsible for lateral heterogeneity in protein distribution of cell plasma membranes, as well as the endoplasmic reticulum and other membranes. We also investigated the influence of two evolutionary cholesterol precursors, desmosterol and lanosterol, on DPPC diffusion to gain deeper insight into those interactions. In a recently published animal study which received much attention, a generation of knock-out mice, which entirely lacked cholesterol, showed surprisingly mild phenotype changes (13). The cell membranes of these animals contained desmosterol, the direct precursor of cholesterol in the biosynthesis pathway. It has been shown previously that desmosterol is similar to cholesterol in its effect on lipid condensation, whereas lanosterol, a more distant precursor of cholesterol, had a significantly smaller effect (14).

We employed a new spectroscopic approach to study lateral lipid diffusion, ^{1}H magic angle spinning (MAS) NMR with application of pulsed field gradients (PFG). In this experiment the high resolution of membrane resonances afforded by MAS is combined with PFG to investigate diffusion of lipids (15–17), embedded small molecules (16,18), and peptides (19). PFG MAS NMR does not require special labeling of the investigated molecules, which may alter molecular properties (20) and can influence diffusion

Submitted February 25, 2005, and accepted for publication July 6, 2005.

Address reprint requests to Klaus Gawrisch, Tel.: 301-594-3750; Fax: 301-594-0035; E-mail: gawrisch@helix.nih.gov.

0006-3495/05/10/2504/09 $2.00

doi: 10.1529/biophysj.105.062018

rates. In addition, no complex sample preparation is required as for application of PFG NMR on oriented samples.

PFG MAS NMR reports the statistics of the translational lipid movement over a certain distance that depends on the diffusion time. Diffusion measurements conducted as a function of diffusion time may reveal properties of membrane structure. For example, lipid diffusion may become diffusion time dependent if the boundaries of domains or clusters are encountered in the specified diffusion time. Therefore, changes in apparent diffusion rates may reflect the size of domains (see, e.g., Polozov and Gawrisch (15)). In addition, the changes in apparent diffusion rates measured at longer diffusion time reflect the finite size of multilamellar liposomes.

In this investigation, we followed the known composition and temperature dependence of phase transitions in cholesterol-DPPC mixtures (21). Since the experiments were conducted on deuterated lipids, we used the opportunity to link ^{2}H NMR and ^{1}H MAS NMR spectral properties to the l_o-l_d/l_o-s_o phase transition isotherm. The diffusion study on cholesterol-, desmosterol-, and lanosterol-containing membranes revealed that the smaller sterols move at somewhat higher rates of lateral diffusion in the lipid matrix than DPPC. The difference was most prominent in membranes containing lanosterol, a sterol that is known to have weaker interactions with phospholipids. For cholesterol we obtained evidence for existence of domains with submicrometer dimensions in the s_o-l_o phase coexistence region.

MATERIALS AND METHODS

Sample preparation

1,2-Dipalmitoyl-d_{62}-*sn*-glycero-3-phosphocholine (DPPC-d_{62}) and cholesterol were purchased from Avanti Polar Lipids (Alabaster, AL). Desmosterol and lanosterol were purchased from Sigma (St. Louis, MO). Lipid and sterols were mixed in chloroform and dried as a thin film under a stream of nitrogen. After additional drying in high vacuum, 50 wt % D_2O for ^{1}H MAS NMR or 50 wt % deuterium-depleted H_2O for ^{2}H NMR measurements were added to form multilamellar vesicles. Samples were homogenized by vortexing and centrifugation; ~15 μL of the liposome dispersion were transferred into 4 mm high resolution MAS rotors fitted with spherical Kel-F inserts for liquid samples or into glass vials for static ^{2}H NMR experiments and frozen at −20°C before the experiments.

^{2}H NMR measurements

^{2}H NMR spectra were recorded on a Bruker DMX300 spectrometer (Bruker BioSpin, Billerica, MA) at a resonance frequency of 46.1 MHz using a 4 mm solenoid coil. Sample temperature was controlled to ±0.1 K and calibrated to within ±0.5 K. The ^{2}H NMR spectra were accumulated using a quadrupolar echo sequence (22) with a relaxation delay of 0.2 s. The two 2.2 μs $\pi/2$ pulses were separated by a 50 μs delay. The carrier frequency was placed in the center of the spectrum. After phase correction to minimize the intensity in the imaginary channel, the data points in the free induction decay (FID) were approximated by a spline function to determine the exact location of the echo maximum with a resolution of 1/10th of the dwell time unit. The FID was time base corrected to begin exactly at the echo maximum, and the spectra were calculated using a Fourier transformation without additional phase correction. An exponential line broadening of 100 Hz was applied. The first moment of the ^{2}H NMR spectra was calculated according to

$$M_1 = \int_{-\infty}^{\infty} |\omega| I(\omega)\, \mathrm{d}\omega \Big/ \int_{-\infty}^{\infty} I(\omega) \mathrm{d}\omega, \qquad (1)$$

where $\omega = 0$ is the center of the spectrum. The limits for the M_1 integration were chosen to cover the full spectral width of the anisotropic resonances.

^{1}H MAS NMR measurements

^{1}H MAS NMR experiments were carried out on a Bruker DMX500 wide bore spectrometer equipped with a 4 mm high resolution MAS probe with a magic angle gradient. Experiments were conducted at a spinning frequency of 5.5 kHz and a typical $\pi/2$ pulse lengths of 4 μs. For comparison of spectra from different samples recorded as a function of temperature, the intensity of resonances was divided by the intensity recorded at the highest temperature.

Temperature and gradient strength were calibrated as described in Gaede and Gawrisch (16). In brief, up to a spinning frequency of 6 kHz we observed sample temperatures slightly below the temperature of the bearing gas due to the Joule-Thompson effect. At higher spinning frequencies, not employed in this investigation, sample temperature increased due to friction in the bearing. We also measured the influence from application of PFGs on sample temperature and found that it was negligible.

For the PFG NMR measurements, a stimulated echo sequence (23) with trapezoidal-shaped bipolar gradient pulses with a length of 5 ms was applied. The effective gradient strength was varied in 16 increments from 0.01 to 0.556 T/m. A longitudinal eddy current delay of 5 ms was introduced before acquisition of the FID. The diffusion time, Δ, was 25 ms for the temperature-dependent diffusion measurements or varied in six increments from 25 to 300 ms for measurements as a function of diffusion time. At every gradient strength, 16 or 32 scans were acquired with a recycle delay of 6 s.

Apparent diffusion coefficients, D_{app}, were determined from the plot of peak intensity versus gradient strength according to Gaede and Gawrisch (16):

$$\ln\left(\frac{I}{I_0}\right) = -\frac{2}{3} k D_{app} + \frac{2}{45} (k D_{app})^2, \qquad (2)$$

where I/I_0 is the normalized intensity and $k = 4\gamma^2 g^2 \delta^2 (\Delta - (T/2) - (2\delta/3))$, where γ is the gyromagnetic ratio of protons, g the gradient strength, δ the gradient pulse length, and T the time between the gradient pulses sandwiching π pulses (24).

The radius of curvature, r_{max}, and the true diffusion coefficient, D, were obtained from the diffusion time dependence of the diffusion displacement $r(\Delta) = (2D_{app}\,\Delta)^{-1/2}$ according to Polozov and Gawrisch (15) and Gaede and Gawrisch (16):

$$r(\Delta) = r_{max} \sin\left(\frac{\sqrt{2D\Delta}}{r_{max}}\right). \qquad (3)$$

RESULTS

Phase behavior of cholesterol-DPPC membranes

Knowledge of the DPPC-cholesterol phase diagram is required for the interpretation of diffusion results. ^{2}H NMR measurements were conducted to ensure that phase behavior of our samples corresponded to published phase diagrams (21). Fig. 1 shows the temperature dependence of the first spectral moment of the ^{2}H NMR spectra as a function of cholesterol concentration. The gel to liquid phase transition is reflected as a drastic increase of the first spectral moment near 311 K. With increasing cholesterol content, the transition width increased and the transition amplitude

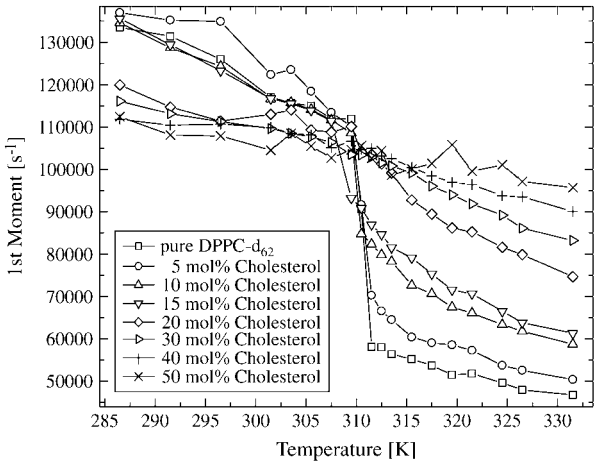

FIGURE 1 Temperature dependence of the ^{2}H NMR first spectral moment of DPPC-d_{62} as a function of cholesterol concentration. Samples were hydrated to 50 wt % H_2O.

decreased. The phase transition completely vanished at cholesterol concentrations above 30 mol %.

At temperatures below 311 K, the first moments fall into two categories with a transition at a cholesterol concentration near 15 mol %. We assume that at low cholesterol concentrations the transition from high to low temperature reflects a l_d-s_o transition, whereas at higher concentrations a l_d-l_o/l_o-s_o transition is detected. We observed these transitions at somewhat elevated cholesterol concentrations compared to previously published phase diagrams (21,25).

The same phase behavior is also reflected in the plot of the normalized ^{1}H MAS NMR resonance intensities of DPPC and cholesterol (Fig. 2). The temperature dependence of the choline γ resonance ($N(CH_3)_3$) can be sorted into three families. The transition is narrowest for cholesterol concentrations from 0 to 15 mol % and becomes significantly wider from 20 to 30 mol %. At concentrations above 30 mol %, broadening takes place at significantly lower temperatures. Up to 15 mol % this signal intensity change is a reflection of an l_d/s_o transition, and from 15 to 30 mol % it indicates an l_d-l_o/l_o-s_o transition. At higher cholesterol concentrations no transition is observed. The broad decrease in resonance intensity that takes place at much lower temperatures is most likely a reflection of the gradual immobilization of lipids in the l_o phase. The behavior of methyl resonance intensities of cholesterol (marked in Fig. 3) as a function of cholesterol content and temperature is very similar, but the low temperature end of the transition is not as well defined in those spectra (Fig. 2 *B*).

Lipid diffusion in cholesterol-DPPC membranes

Fig. 3 shows the ^{1}H MAS NMR spectra at 324 K of pure DPPC-d_{62} and of DPPC-d_{62} mixed with 20 mol % sterol. The headgroup choline resonance (marked with 5*) was chosen for the analysis of the DPPC diffusion because it has

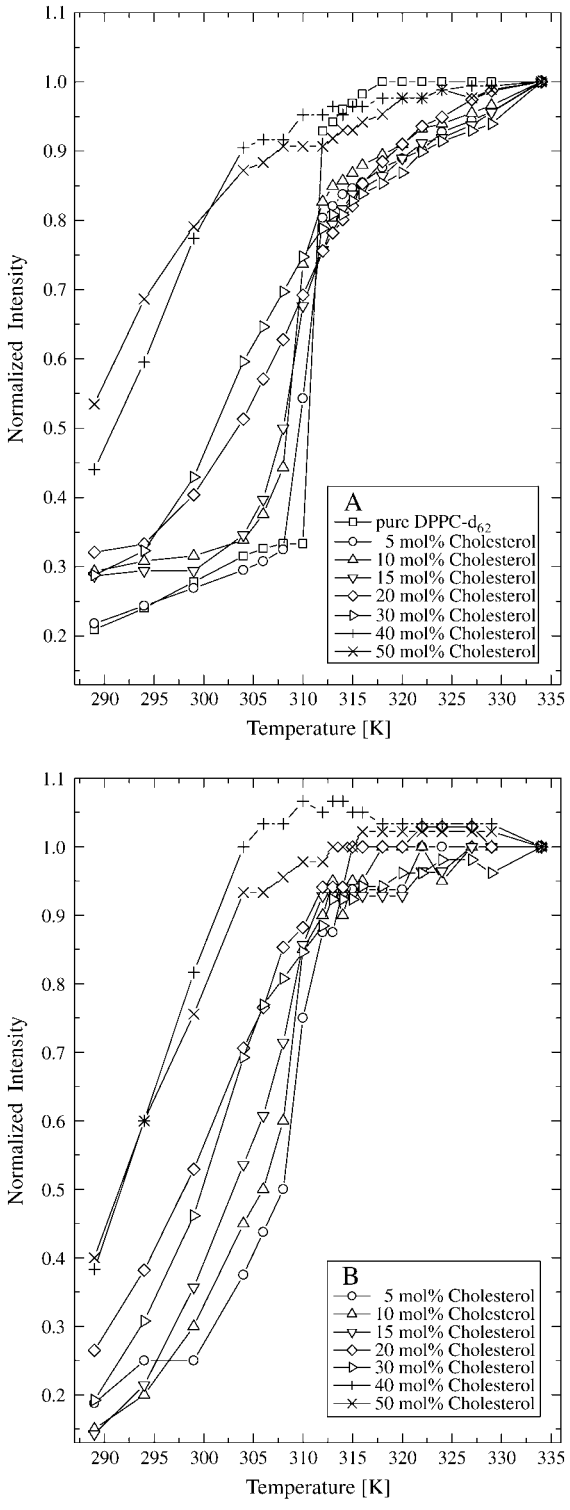

FIGURE 2 Temperature dependence of the normalized ^{1}H MAS NMR resonance intensities of (*A*) the DPPC-d_{62} choline γ signal and (*B*) the methyl signal of cholesterol (marked in Fig. 3) as a function of cholesterol concentration. Samples were hydrated to 50 wt % D_2O.

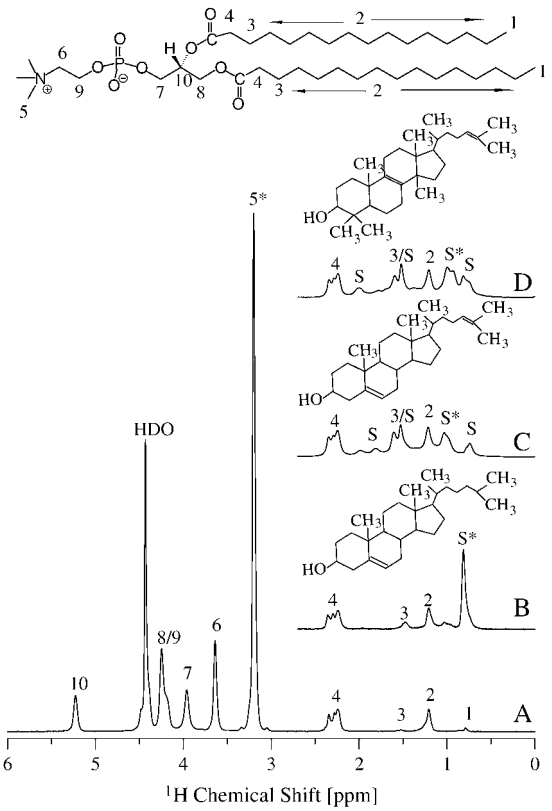

FIGURE 3 ^{1}H MAS NMR spectra of pure DPPC-d_{62} (*A*) and the upfield region of these spectra in the presence of 20 mol % (*B*) cholesterol, (*C*) desmosterol, and (*D*) lanosterol at a temperature of 324 K and a MAS frequency of 5.5 kHz. The molecular structures as well as the lipid resonance assignment are given above the respective spectra. Signals used for intensity and diffusion analysis are marked by an asterisk. Sterol signals are marked by *S*. Samples were hydrated to 50 wt % D_2O.

no superposition with sterol resonances and very high signal intensity. The marked methyl resonances (*S**) of sterols were chosen for measurement of sterol diffusion. Sterol resonances that are superimposed on residual proton resonances of DPPC-d_{62} chains (98% deuterated) were not considered.

In Fig. 4, the temperature dependence of the apparent diffusion coefficients of DPPC (*A*) and cholesterol (*B*) as a function of cholesterol concentration in the membrane are shown (see also Supplementary Table 1). At 324 K, lipid diffusion coefficients decrease with increasing cholesterol content with some discontinuity at concentrations corresponding to transitions between the l_d to $l_d + l_o$ to l_o phase regions (Fig. 4 *A*). We observed little reduction in diffusion rates up to 10 mol % cholesterol. In contrast, a significant reduction in diffusion rates with increasing cholesterol content was detected at higher cholesterol concentrations.

From 324 to 311 K, the diffusion rates are very temperature dependent. At temperatures below 311 K, all apparent diffusion rates converge to similar values and show little temperature dependence down to 294 K. When interpreting diffusion results, it must be considered that spectra may represent superposition of phases. Because of

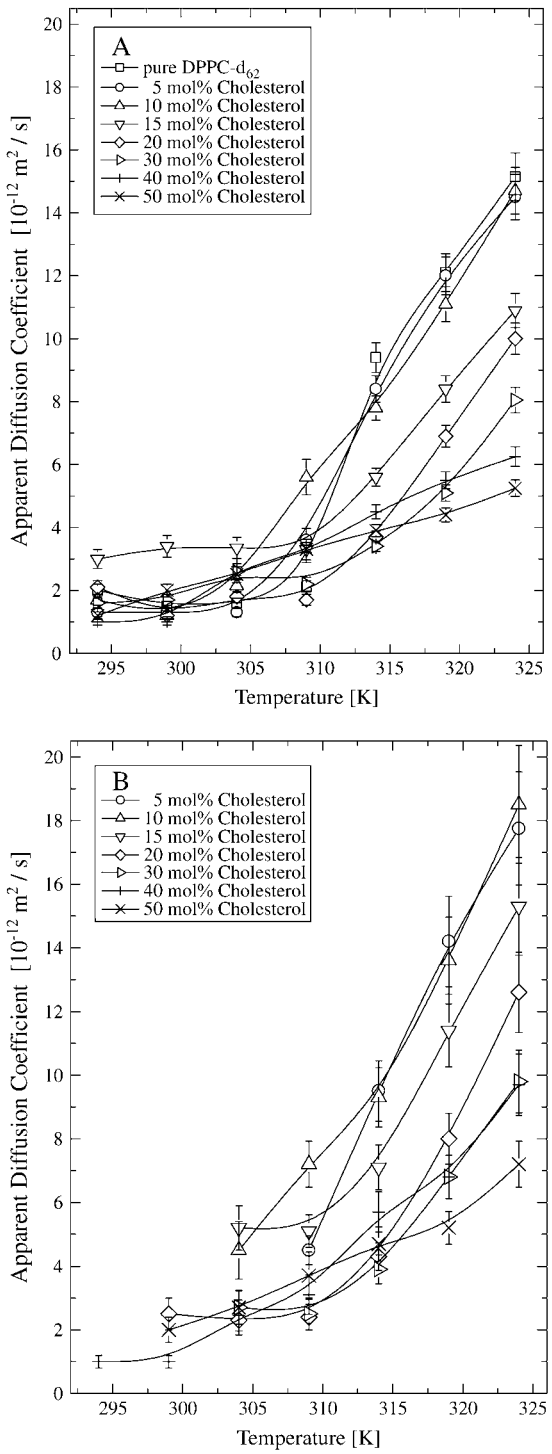

FIGURE 4 Temperature dependence of the apparent diffusion coefficients of (*A*) DPPC-d_{62} and (*B*) cholesterol as a function of cholesterol concentration. All data were recorded at a diffusion time of 25 ms.

signal broadening of DPPC resonances in the gel phase and because of intensity losses due to faster relaxation of gel phase lipid, the diffusion below 311 K reflects almost exclusively diffusion in the remnants of the fluid phase.

The activation energy of lipid diffusion is shown in Fig. 5. It was calculated from an Arrhenius plot of the diffusion coefficients in the temperature range 314–324 K, corresponding to membranes in the l_d, $l_d + l_o$, or l_o phase regions. Activation energies of lateral diffusion increase from 38 kJ/mol for pure DPPC to 70 kJ/mol for the $l_d + l_o$ phase coexistence region and decrease again to ~55 kJ/mol for the l_d phase. Diffusion rates of cholesterol (Fig. 4 *B*) and activation energies of cholesterol lateral diffusion (Fig. 5) mirror the DPPC behavior. However, cholesterol diffuses somewhat faster and has slightly higher activation energies. This is most evident at higher temperature where cholesterol activation energies exceed the lipid values by 10 kJ/mol. Below 311 K, cholesterol diffusion rates more closely resemble the lipid diffusion values. Typical experimental errors of DPPC diffusion constants are 5% at high temperatures and somewhat larger at temperatures below 311 K due to lower signal intensity. Experimental errors of cholesterol diffusion rates are about a factor of 2 larger because of the lower signal intensities of cholesterol resonances.

To investigate the influence of vesicle curvature or possible domain formation on apparent diffusion rates, the diffusion displacement $r = (2D_{app}\,\Delta)^{-1/2}$ was measured as a function of diffusion time Δ. Fig. 6 shows a typical data set (20 mol % cholesterol in DPPC-d_{62} recorded at 324 K and 304 K). At both temperatures the data could be well approximated by the model, assuming lateral diffusion over spheres (16,26). The data analysis yielded a curvature-corrected true lateral diffusion rate and an effective radius of curvature. At 324 K the radii for all investigated samples (see Supplementary Table 2) are in the range from 1.5 to 3.0 μm, which is typical for fully hydrated multilamellar liposomes (15,16).

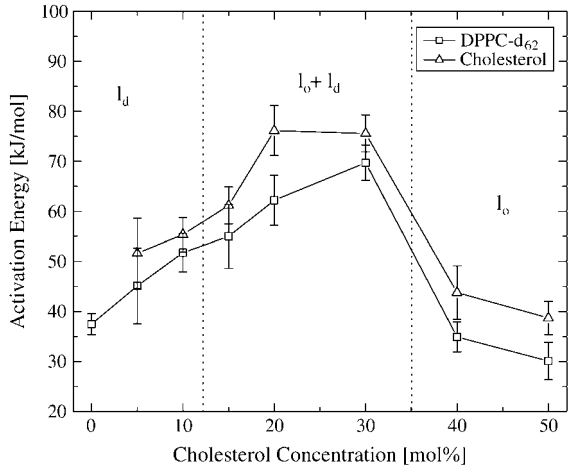

FIGURE 5 Activation energies of DPPC-d_{62} (□) and cholesterol (△) diffusion obtained from Arrhenius plots in the temperature range from 314 K to 324 K. The dotted lines represent the approximate location of the phase boundaries.

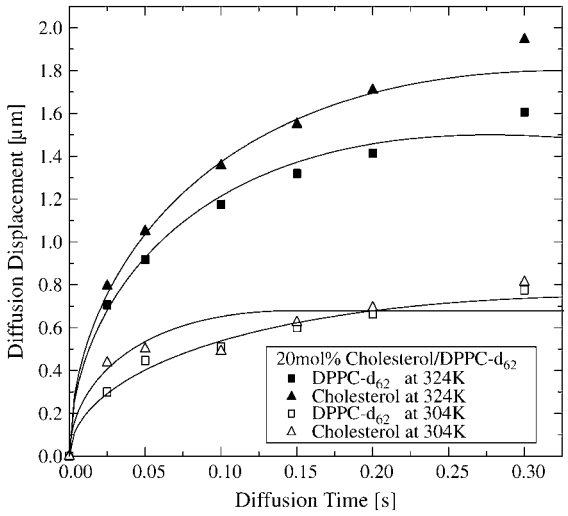

FIGURE 6 Diffusion time dependence of the diffusion displacement for DPPC-d_{62} (*squares*) and cholesterol (*triangles*) at 20 mol % cholesterol/DPPC-d_{62} measured at a temperature of 324 K (*solid symbols*) and 304 K (*open symbols*). The lines represent the best fit to Eq. 3.

At 304 K and cholesterol concentrations below 15 mol %, membranes are predominantly in the s_o state. However, the lipid signals most likely are dominated by remnants of the fluid phase. At this temperature we observed effective radii in the range from 0.3 to 0.4 μm. This is far less than the effective liposome radii of 1.7–2.2 μm measured at higher temperatures (324 K). True diffusion rates of lipids at 304 K are ~1 order of magnitude lower than at 324 K. At 304 K and cholesterol concentrations in the range 15–30 mol % the difference in effective radii to liposome radii (measured at 324 K) is somewhat smaller, and true lipid diffusion rates between high and lower temperatures differ only by a factor of 3. At cholesterol concentrations higher than 30 mol %, effective radii and curvature-corrected lipid diffusion rates differ by a factor of 2.

Diffusion in desmosterol- and lanosterol-containing membranes

Several studies using DSC and NMR spectroscopy as well as computer simulations suggested that the $l_d + l_o$ coexistence region is completely absent in lanosterol-containing membranes (25,27,28). The temperature dependence of the first moment of DPPC-d_{62} in the presence of 20 mol % of the respective sterol is shown in Fig. 7. At high temperatures, the first moments are highest for the cholesterol-containing sample, followed by desmosterol, and lanosterol. Below 311 K, cholesterol and desmosterol samples have similar first moments, whereas the first moments for lanosterol are higher.

The phase transition temperature remains at 311 K in the presence of all sterols. However, the width and amplitudes of the spectral changes are different. The cholesterol-containing

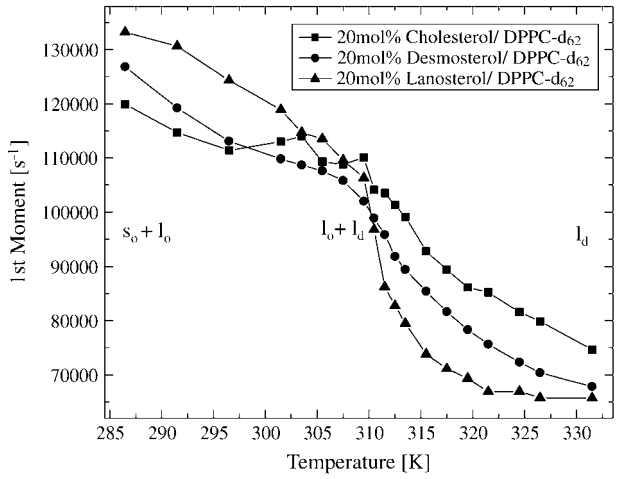

FIGURE 7 Temperature dependence of the first spectral moment determined from ^{2}H NMR spectra of DPPC-d_{62} in the presence of (■) 20 mol % cholesterol, (●) 20 mol % desmosterol, and (▲) 20 mol % lanosterol. Samples were hydrated to 50 wt % H_2O.

sample has the smallest jump and the widest transition. Lanosterol has a rather sharp transition of large amplitude, which is likely a result of the attenuated effect of lanosterol on lipid condensation as reported in Huster et al. (14). Desmosterol has a phase transition width similar to cholesterol, but the amplitude of spectral changes is larger.

The ^{1}H MAS NMR lipid and sterol resonance intensities (Fig. 8) show a phase transition midpoint at 311 K, which is consistent with the ^{2}H NMR data. Sterol resonance intensity as a function of temperature is constant up to 314 K and drops rapidly at the onset of the transition. The region of intensity changes of cholesterol is slightly wider and asymmetric toward low temperatures.

Fig. 9 shows the temperature dependence of the apparent diffusion coefficients of DPPC-d_{62} (*A*) and the three sterols (*B*) at a concentration of 20 mol % (see also Supplementary Table 1). For all three sterols at temperatures above the phase transition, DPPC diffusion rates in mixed samples are lower than in pure DPPC. Addition of desmosterol and lanosterol resulted in a similar reduction (Fig. 9 *A*), whereas rates are somewhat lower for the cholesterol-containing sample. Below the phase transition, the DPPC diffusion rates are similar for all three sterols and show little temperature dependence. Again, those rates most likely represent diffusion in the remnants of the fluid phase.

The diffusion rates of the three sterols displays larger differences (see Fig. 9 *B*). Lanosterol has twofold higher diffusion rates than cholesterol, whereas desmosterol rates are intermediate between the two. Diffusion measurements conducted as a function of diffusion time yielded comparable liposome radii of 1.5–2.5 μm (measured at 324 K) for all three sterols and effective radii in the range from 0.5 to 0.9 μm at 304 K.

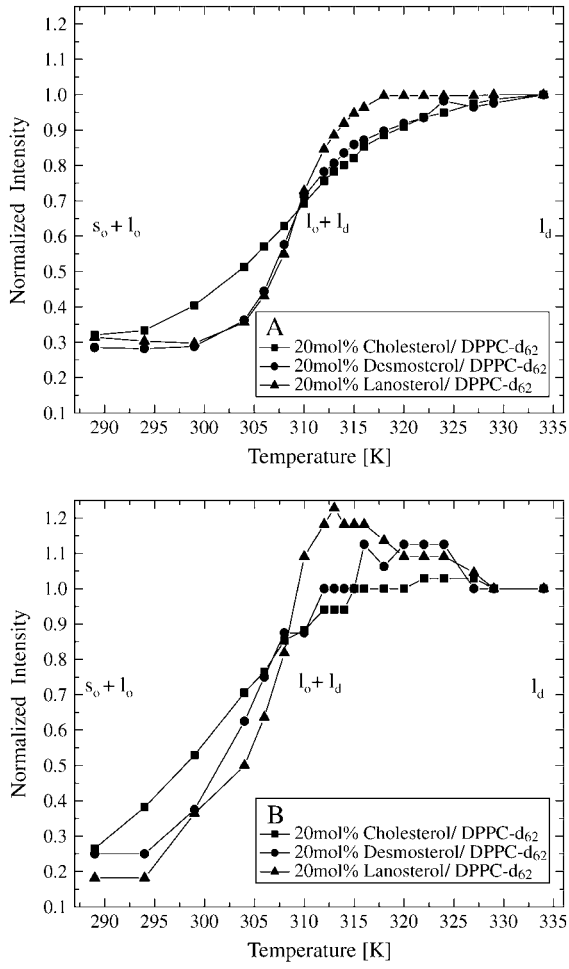

FIGURE 8 Temperature dependence of the ^{1}H MAS NMR resonance intensities of (*A*) the DPPC-d_{62} choline γ signal and (*B*) the methyl signal of the sterols (marked in Fig. 3) for samples containing (■) 20 mol % cholesterol, (●) 20 mol % desmosterol, and (▲) 20 mol % lanosterol. Samples were hydrated to 50 wt % D_2O.

DISCUSSION

The lateral diffusion of three sterols and DPPC in mixed membranes was investigated by a novel approach, ^{1}H PFG MAS NMR spectroscopy. The method combines the high resolution of MAS resonances with the opportunity to measure diffusion rates for every substance in the mixture, e.g., lateral diffusion of both sterol and phospholipid in the same membrane. NMR diffusion measurements do not require perturbing labels. This is particularly important for diffusion measurements on small molecules like lipids. We have shown previously that introduction of such labels may perturb membrane properties (20).

It was observed that cholesterol diffusion in the l_d, $l_d + l_o$, and l_o phases is slightly faster than DPPC diffusion at all cholesterol concentrations. Higher rates of sterol diffusion were expected because of the lower molecular weight compared to DPPC. The small magnitude of differences

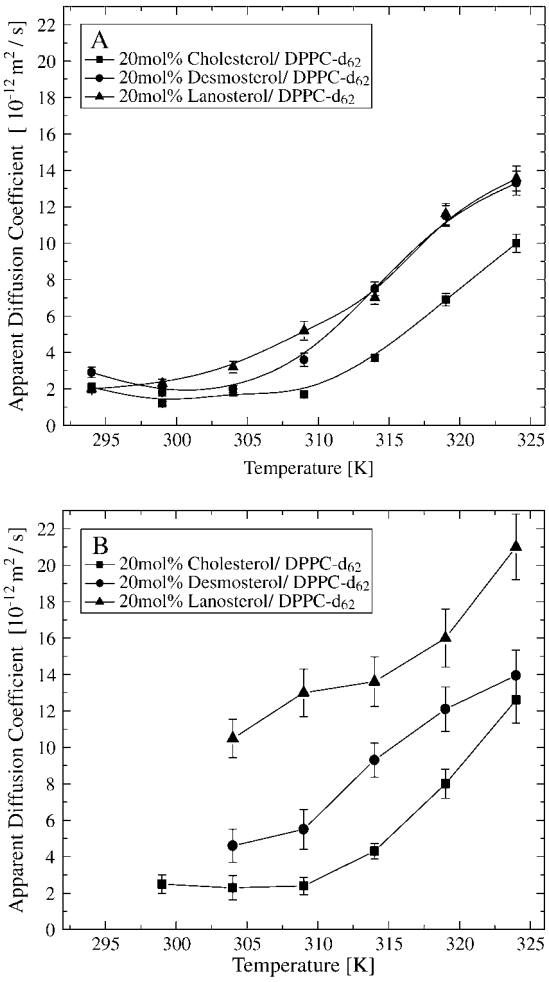

FIGURE 9 Temperature dependence of the apparent diffusion coefficients of (*A*) DPPC-d_{62} and (*B*) the sterols in samples containing (■) 20 mol % cholesterol, (●) 20 mol % desmosterol, and (▲) 20 mol % lanosterol. All data were recorded at a diffusion time of 25 ms.

suggests existence of strong but transient interactions between cholesterol and DPPC. In a PFG NMR study on oriented cholesterol/1,2-dimyristoyl-*sn*-glycero-3-phosphocholine (DMPC) membranes using fluorinated cholesterol, equal diffusion rates of DMPC and cholesterol were observed (29). Most likely, the differences in diffusion rates are even smaller for DMPC with shorter hydrocarbon chains, or cholesterol diffusion rates were influenced by fluorination that was used to obtain a distinct cholesterol resonance.

DPPC and sterol diffusion rates in the lanosterol- and desmosterol-containing samples were higher, and lanosterol diffusion rates significantly exceeded the DPPC rates. These observations confirm that cholesterol induces the tightest lipid packing, which is also reflected in the highest chain order parameters (14). The results are also in agreement with the significant differences in properties between cholesterol- and lanosterol-containing membranes as determined by ^{2}H NMR relaxation measurements (30) or by micromechanical measurements (31).

The apparent weaker interaction between lanosterol and DPPC compared to cholesterol and DPPC must be related to the molecular structure of lanosterol. This sterol has two additional methyl groups at carbon C4, very close to the hydroxyl group that is responsible for the amphipathic character of sterols. Their presence may weaken the ability of lanosterol to form hydrogen bonds to phospholipids. Furthermore, the difference in the location of the double bond in the sterol ring system could be important. It was reported that the α-surface of lanosterol is less planar, which may weaken van der Waals interactions between lipid hydrocarbon chains and lanosterol (32–34). Last but not least, the methyl group in position C14 of lanosterol may result in additional packing constraints at the sterol surface (28). In contrast, desmosterol and cholesterol differ only by a double bond in the flexible hydrocarbon tail region. Consequently, differences in properties between cholesterol- and desmosterol-containing samples are much smaller.

We observed an increase of activation energies of cholesterol and lipid lateral diffusion with increasing cholesterol content in the l_d phase, and particularly in the $l_d + l_o$ phase coexistence region. Activation energies in the l_o state are lower again. The activation energies for pure l_d and l_o states reflect potentials of DPPC-sterol association. The much higher activation energies in the $l_d + l_o$ phase coexistence region could be the result of DPPC and sterol diffusion across domain boundaries.

Diffusion measurements conducted as a function of diffusion time at temperatures above 311 K yielded effective liposome radii in the lower micrometer range, which is typical for lipids at this water content. We observed such values also at cholesterol concentrations for which coexistence of l_d and l_o domains was reported. This indicates that the boundaries of coexisting l_d and l_o domains are not insurmountable barriers for lipid diffusion. The cholesterol dependence of DPPC and cholesterol activation energies is very similar, but values for cholesterol are always higher by 5–10 kJ/mol. Perhaps this is a reflection of an additional activation energy related to DPPC-sterol interaction that is present at all concentrations.

In studies by the Lindblom lab (35,36), the influence of cholesterol concentration on diffusion of 1,2-dioleoyl-*sn*-glycero-3-phosphocholine (DOPC), 1-palmitoyl-2-oleoyl-*sn*-glycero-3-phosphocholine (POPC), DMPC, and SM was investigated by PFG NMR on oriented samples. Our results are similar to the diffusion in SM/cholesterol mixtures reported in Filippov et al. (36), which confirms that DPPC and SM are structurally very close. At high (40 mol %) cholesterol content in cholesterol/DPPC membranes, comparable lateral diffusion coefficients for cholesterol were measured by quasielastic neutron scattering (37). Also, somewhat higher diffusion coefficients for lanosterol were observed by this method (38). However the differences between cholesterol and lanosterol were smaller than in this

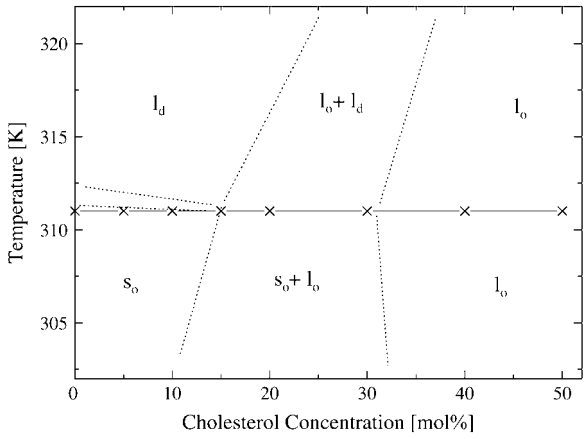

FIGURE 10 Schematic phase diagram of DPPC-cholesterol mixtures. The location of phase boundaries is valid at temperatures near 311 K only. The phases were assigned according to the phase diagram by Vist and Davis (21).

study. The temperature and sterol concentration dependence of DPPC diffusion of cholesterol and lanosterol samples is in agreement with qualitative predictions from Monte Carlo simulations by Polson et al. (25).

At temperatures below 311 K, we observed that lipid diffusion is restricted to regions with effective radii significantly smaller than liposome size. This must be a reflection of domain formation. Because signal intensity at those temperatures stems primarily from residual amounts of fluid lipids, this is the effective size of fluid domains. It is intriguing that the diffusion time dependence for even the smallest domains fits to the equation for round liposomes rather than to a model of flat domains in a larger liposome. This is very suggestive for the formation of spherical, raspberry-like domains much smaller than liposome size.

The experiments conducted in this study mostly confirmed the previously reported DPPC-cholesterol phase diagram (21,25) except for minor corrections in the location of phase boundaries as indicated in Fig. 10. At 311 K the transition from l_d to $l_d + l_o$ takes place at a cholesterol concentration near 15 mol %, and the transition from $l_d + l_o$ to l_o was detected at a cholesterol concentration at or slightly above 30 mol %.

In conclusion, the boundaries between liquid-ordered and liquid-disordered domains are not insuperable barriers for phospholipid and sterol diffusion. However, activation energies of lateral diffusion in the phase coexistence region strongly increased, suggesting that some kind of barrier to diffusion exists. Sterol diffusion rates are strictly dependent on sterol affinity to phospholipids, with cholesterol showing stronger interactions and lower diffusion rates.

SUPPLEMENTARY MATERIAL

An online supplement to this article can be found by visiting BJ Online at http://www.biophysj.org.

This research was supported by the Intramural Research Program of the National Institutes of Health, National Institute on Alcohol Abuse and Alcoholism and by grants from the Europäischer Fonds für regionale Entwicklung (EFRE 4212/03-12) and the Deutsche Forschungsgemeinschaft (DFG HU 720/5-1)

The study was supported by grants from the Europäischer Fonds für regionale Entwicklung (EFRE 4212/03-12) and the Deutsche Forschungsgemeinschaft (DFG HU 720/5-1).

REFERENCES

1. Demel, R. A., K. R. Bruckdorfer, and L. L. van Deenen. 1972. The effect of sterol structure on the permeability of lipomes to glucose, glycerol and Rb^+. *Biochim. Biophys. Acta*. 255:321–330.
2. Huster, D., K. Arnold, and K. Gawrisch. 1998. Influence of docosahexaenoic acid and cholesterol on lateral lipid organization in phospholipid mixtures. *Biochemistry*. 37:17299–17308.
3. Simons, K., and E. Ikonen. 1997. Functional rafts in cell membranes. *Nature*. 387:569–572.
4. Anderson, R. G., and K. Jacobson. 2002. A role for lipid shells in targeting proteins to caveolae, rafts, and other lipid domains. *Science*. 296:1821–1825.
5. Silvius, J. R. 2003. Role of cholesterol in lipid raft formation: lessons from lipid model systems. *Biochim. Biophys. Acta*. 1610:174–183.
6. Ayala-Sanmartin, J. 2001. Cholesterol enhances phospholipid binding and aggregation of annexins by their core domain. *Biochem. Biophys. Res. Commun*. 283:72–79.
7. Klein, U., G. Gimpl, and F. Fahrenholz. 1995. Alteration of the myometrial plasma membrane cholesterol content with beta-cyclodextrin modulates the binding affinity of the oxytocin receptor. *Biochemistry*. 34:13784–13793.
8. Mitchell, D. C., M. Straume, J. L. Miller, and B. J. Litman. 1990. Modulation of metarhodopsin formation by cholesterol-induced ordering of bilayer lipids. *Biochemistry*. 29:9143–9149.
9. Albert, A. D., J. E. Young, and P. L. Yeagle. 1996. Rhodopsin-cholesterol interactions in bovine rod outer segment disk membranes. *Biochim. Biophys. Acta*. 1285:47–55.
10. Ohvo-Rekila, H., B. Ramstedt, P. Leppimaki, and J. P. Slotte. 2002. Cholesterol interactions with phospholipids in membranes. *Prog. Lipid Res*. 41:66–97.
11. Soubias, O., F. Jolibois, V. Reat, and A. Milon. 2004. Understanding sterol-membrane interactions, Part II: complete ^1H and ^{13}C assignments by solid-state NMR spectroscopy and determination of the hydrogen-bonding partners of cholesterol in a lipid bilayer. *Chemistry*. 10:6005–6014.
12. Brown, D. A., and E. London. 2000. Structure and function of sphingolipid- and cholesterol-rich membrane rafts. *J. Biol. Chem*. 275:17221–17224.
13. Wechsler, A., A. Brafman, M. Shafir, M. Heverin, H. Gottlieb, G. Damari, S. Gozlan-Kelner, I. Spivak, O. Moshkin, E. Fridman, Y. Becker, R. Skaliter, P. Einat, A. Faerman, I. Bjorkhem, and E. Feinstein. 2003. Generation of viable cholesterol-free mice. *Science*. 302:2087.
14. Huster, D., H. A. Scheidt, K. Arnold, A. Herrmann, and P. Müller. 2005. Desmosterol may replace cholesterol in lipid membranes. *Biophys. J*. 88:1838–1844.
15. Polozov, I. V., and K. Gawrisch. 2004. Domains in binary SOPC/POPE lipid mixtures studied by pulsed field gradient ^1H MAS NMR. *Biophys. J*. 87:1741–1751.
16. Gaede, H. C., and K. Gawrisch. 2003. Lateral diffusion rates of lipid, water, and a hydrophobic drug in a multilamellar liposome. *Biophys. J*. 85:1734–1740.
17. Pampel, A., D. Michel, and R. Reszka. 2002. Pulsed field gradient MAS-NMR studies of the mobility of carboplatin in cubic liquid-crystalline phases. *Chem. Phys. Lett*. 357:131–136.

18. Scheidt, H. A., A. Pampel, L. Nissler, R. Gebhardt, and D. Huster. 2004. Investigation of the membrane localization and distribution of flavonoids by high-resolution magic angle spinning NMR spectroscopy. *Biochim. Biophys. Acta.* 1663:97–107.

19. Pampel, A., J. Kärger, and D. Michel. 2003. Lateral diffusion of a transmembrane peptide in lipid bilayers studied by pulsed field gradient NMR in combination with magic angle sample spinning. *Chem. Phys. Lett.* 379:555–561.

20. Scheidt, H. A., P. Müller, A. Herrmann, and D. Huster. 2003. The potential of fluorescent and spin labeled steroid analogs to mimic natural cholesterol. *J. Biol. Chem.* 278:45563–45569.

21. Vist, M. R., and J. H. Davis. 1990. Phase equilibria of cholesterol/dipalmitoylphosphatidylcholine mixtures: ^{2}H nuclear magnetic resonance and differential scanning calorimetry. *Biochemistry.* 29:451–464.

22. Davis, J. H., K. R. Jeffrey, M. Bloom, M. I. Valic, and T. P. Higgs. 1976. Quadropolar echo deuteron magnetic resonance spectroscopy in ordered hydrocarbon chains. *Chem. Phys. Lett.* 42:390–394.

23. Cotts, R. M., M. J. R. Hoch, T. Sun, and J. T. Marker. 1989. Pulsed field gradient stimulated echo methods for improved NMR diffusion measurements in heterogeneous systems. *J. Magn. Reson.* 83:252–266.

24. Fordham, E. J., P. P. Mitra, and L. L. Latour. 1996. Effective diffusion times in multi-pulse PFG diffusion measurements in porous media. *J. Magn. Reson. A.* 121:187–192.

25. Polson, J. M., I. Vattulainen, H. Zhu, and M. J. Zuckermann. 2001. Simulation study of lateral diffusion in lipid-sterol bilayer mixtures. *Eur. Phys. J. E.* 5:485–497.

26. Gaede, H. C., and K. Gawrisch. 2004. Multi-dimensional pulsed field gradient magic angle spinning NMR experiments on membranes. *Magn. Reson. Chem.* 42:115–122.

27. Nielsen, M., J. Thewalt, L. Miao, J. H. Ipsen, M. Bloom, M. J. Zuckermann, and O. G. Mouritsen. 2000. Sterol evolution and the physics of membranes. *Europhys. Lett.* 52:368–374.

28. Miao, L., M. Nielsen, J. Thewalt, J. H. Ipsen, M. Bloom, M. J. Zuckermann, and O. G. Mouritsen. 2002. From lanosterol to cholesterol: structural evolution and differential effects on lipid bilayers. *Biophys. J.* 82:1429–1444.

29. Orädd, G., G. Lindblom, and P. W. Westerman. 2002. Lateral diffusion of cholesterol and dimyristoylphosphatidylcholine in a lipid bilayer measured by pulsed field gradient NMR spectroscopy. *Biophys. J.* 83:2702–2704.

30. Martinez, G. V., E. M. Dykstra, S. Lope-Piedrafita, and M. F. Brown. 2004. Lanosterol and cholesterol-induced variations in bilayer elasticity probed by H-2 NMR relaxation. *Langmuir.* 20:1043–1046.

31. Endress, E., S. Bayerl, K. Prechtel, C. Maier, R. Merkel, and T. M. Bayerl. 2002. The effect of cholesterol, lanosterol, and ergosterol on lecithin bilayer mechanical properties at molecular and microscopic dimensions: a solid-state NMR and micropipet study. *Langmuir.* 18:3293–3299.

32. Xu, X., and E. London. 2000. The effect of sterol structure on membrane lipid domains reveals how cholesterol can induce lipid domain formation. *Biochemistry.* 39:843–849.

33. Child, P., and A. Kuksis. 1983. Critical role of ring structure in the differential uptake of cholesterol and plant sterols by membrane preparations in vitro. *J. Lipid Res.* 24:1196–1209.

34. Wang, J., Megha, and E. London. 2004. Relationship between sterol/steroid structure and participation in ordered lipid domains (lipid rafts): implications for lipid raft structure and function. *Biochemistry.* 43:1010–1018.

35. Filippov, A., G. Orädd, and G. Lindblom. 2003. Influence of cholesterol and water content on phospholipid lateral diffusion in bilayers. *Langmuir.* 19:6397–6400.

36. Filippov, A., G. Orädd, and G. Lindblom. 2003. The effect of cholesterol on the lateral diffusion of phospholipids in oriented bilayers. *Biophys. J.* 84:3079–3086.

37. Gliss, C., O. Randel, H. Casalta, E. Sackmann, R. Zorn, and T. Bayerl. 1999. Anisotropic motion of cholesterol in oriented DPPC bilayers studied by quasielastic neutron scattering: the liquid-ordered phase. *Biophys. J.* 77:331–340.

38. Endress, E., H. Heller, H. Casalta, M. F. Brown, and T. M. Bayerl. 2002. Anisotropic motion and molecular dynamics of cholesterol, lanosterol, and ergosterol in lecithin bilayers studied by quasi-elastic neutron scattering. *Biochemistry.* 41:13078–13086.